Sensory Responses in Solution vs Solid State: A Fluorescence Quenching Study of Poly(iptycenebutadiynylene)s

Dahui Zhao and Timothy M. Swager*

Department of Chemistry, Massachusetts Institute of Technology, Cambridge, Massachusetts 02139

Received July 20, 2005

ABSTRACT: A new series of poly(*p*-phenylenebutadiynylene)s has been synthesized with unique polymer structural features. In these systems each of the *p*-phenylene units in the conjugated backbone is the core of a rigid three-dimensional iptycene scaffold. The fluorescence quenching properties of these polymers in response to a series of electron-deficient aromatic compounds have been investigated in both solution and the solid state. It was found that in solution these polymers displayed higher quenching sensitivity toward studied quenchers compared to a more open-structure iptycene-containing poly(*p*-phenyleneethynylene). The quenching behaviors of the conjugated polymer were shown to be strongly influenced by the configuration of the incorporated iptycences. The thin films investigations revealed differences in both the fluorescence quenching and the recovery processes. Distinct behaviors indicated that the fluorescence quenching in the solid state is dictated by different factors than those in solution. Our results further suggest that poly(*p*-phenylenebutadiynylene)s containing large iptycene scaffolds that introduce porosity have the ability to efficiently sequester the quencher molecules within thin films as these materials display slow fluorescence recoveries.

Introduction

Fluorescent conjugated polymers have demonstrated great utility and high sensitivity in chemical and biological sensor schemes.[1−3] The superior performance of these polymers arises as a benefit from the "molecular wire" effect;[4] i.e., the conjugated polymer backbone allows efficient electron delocalization and exciton migration over large distances, thereby creating amplified sensory responses compared to small-molecule-based sensors.[1] An additional advantage of using polymers as sensor materials emerges from the modular nature of polymers; i.e., the structure and sequence of the repeating units within polymers can be widely varied and modified, which allows the polymers to be tailored to suit for diverse targets and potentially achieve high selectivity.

Previous reports from our laboratory detailed a highly efficient chemosensory material for the detection of nitroaromatic explosive TNT (2,4,6-trinitrotoluene) by taking advantage of the ultrasensitive fluorescent quenching property of poly(*p*-phenyleneethynylene)s (PPEs).[5] Upon introducing pentiptycene units into the PPE polymer, the photoluminescence stability and solid state quantum yields were greatly increased, and these improvements were ascribed to the "insulating" function of the pentiptycene units. In effect, the three-dimensional, noncompliant iptycene structures sterically isolate the polymer backbones and thereby reduced intermolecular electron/orbital coupling and the self-quenching that usually accompanies these interactions. In addition, rigid elaborated scaffolds can also introduce additional free volume in the solid-state material, thereby facilitating rapid analyte diffusion into the polymer film to achieve faster and larger amplitude responses.[6,7]

Our ongoing efforts are directed at improving the performance of the existing sensors in terms of selectivity and sensitivity as well as discovering new sensory materials for different targets. Poly(*p*-phenylenebutadiynylene)s (PPDs) have similar electronic and photophysical properties as PPEs[8] and therefore may be expected to exhibit comparable fluorescence quenching properties. Nevertheless, the synthesis of PPDs enjoys an important advantage over PPEs in that they can be generated from homocoupling of synthetically readily accessible monomers having two terminal acetylene groups. This allows PPDs to be prepared with high molecular weight (MW) without a need for rigorous comonomer stoichiometry control as required in PPE syntheses. As mentioned earlier, since the iptycene units play an important role in attaining optimal sensory performance for the solid-state PPEs, incorporating iptycene units into PPDs was considered desirable in our initial development of PPD-based sensors.

On the basis of the above considerations, a series of poly(*p*-phenylenebutadiynylene)s (PPDs), **P1**−**3**, were designed. These polymers have iptycenes of different size and shape installed in each repeating unit and therefore will also be referred to as poly(iptycenebutadiynylene)s in the following discussion. The appended alkoxy side chains were expected to impart adequate solubility for convenient polymer synthesis and subsequent solution processing. We have taken a systematic approach to investigating these PPDs in regard to their fluorescence quenching responses to a series of electron-deficient aromatic compounds including TNT. The quenching properties of these polymers were compared to that of a pentiptycene-containing PPE, **P4**, which is the previously optimized TNT sensing material.[5] These results are to be reported in this contribution.

It is noteworthy that for **P1**−**3** every *p*-phenylene unit within the conjugated backbone is built into an iptycene structure as the core unit. As a result of this restrictive spatial arrangement, direct cofacial interactions between bulky nitroaromatic molecules and the polymer's backbone are limited. This unique feature represents a key difference between these PPDs and the previously studied PPEs (e.g., **P4**). In the latter, half of the

* Corresponding author. E-mail: tswager@mit.edu.

10.1021/ma051584y CCC: $30.25
Published on Web 10/05/2005

Scheme 1. Syntheses of P1−3 and the Structure of P4[a]

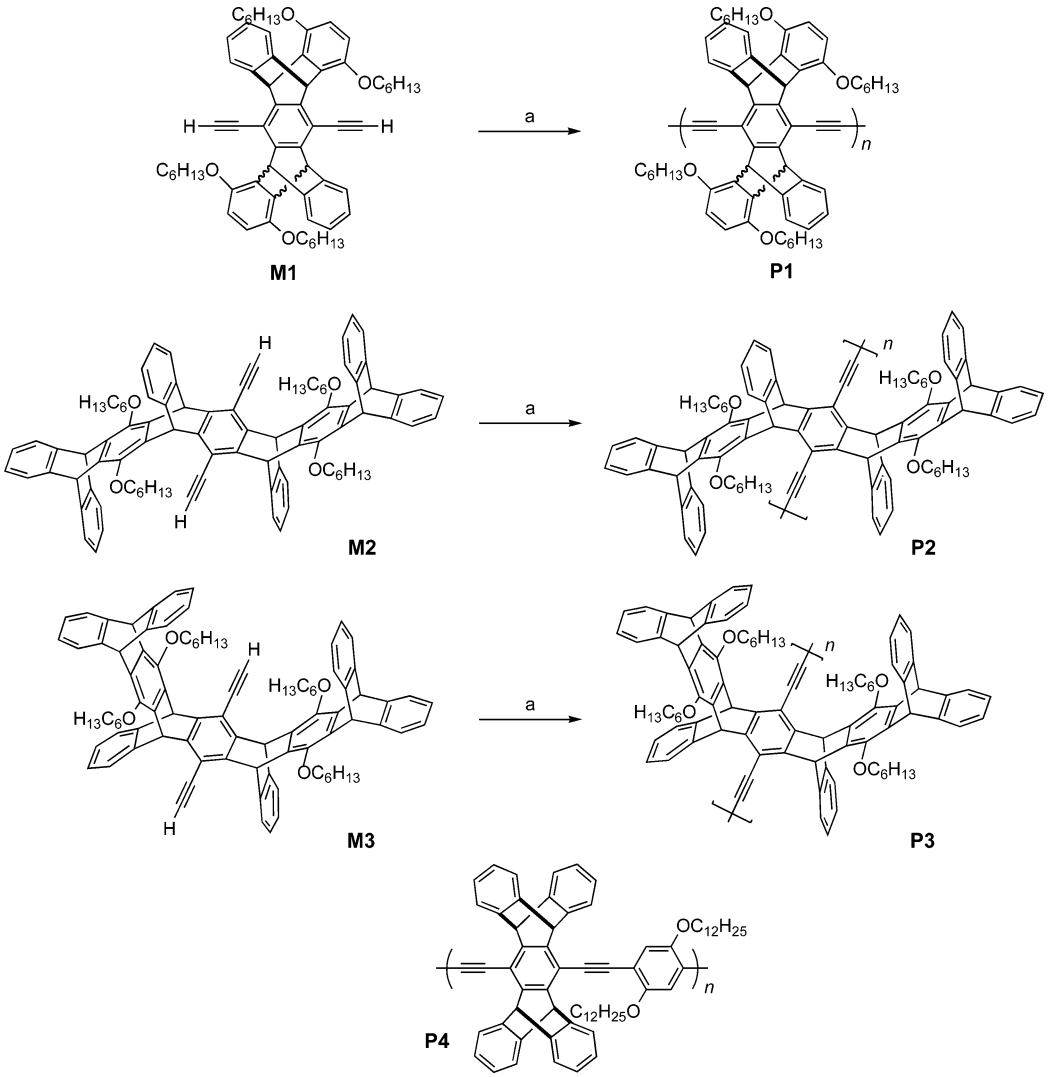

[a] Reagents and conditions: (a) $Pd(PPh_3)_4$, CuI, 1,4-benzoquinone, diisopropylamine/toluene (3:7, v/v), 60 °C, 3 days.

conjugated phenyl rings in the backbone were not integrated as part of pentiptycenes and therefore available to engage in strong unrestricted cofacial $\pi-\pi$ stacking with complementary arenes. This difference is envisioned to provide insightful information on the quenching mechanism of the conjugated polymers, namely whether an intimate cofacial π-stacking between the polymer backbone and the quencher molecule is essential for efficient quenching to take place. We were also interested to compare the quenching behaviors of **P1**−**3** side by side to elucidate how the size and geometric configuration of the iptycenes affect the polymer−quencher interactions.

Results and Discussion

Polymer Syntheses. The syntheses of polymers **P1**−**3** are illustrated in Scheme 1. Following the procedure as previously reported and using 1,4-benzoquinone as the oxidative reagent,[8] **P1**−**3** were obtained via Pd-catalyzed polymerizations of corresponding monomers **M1**−**3**,[9] respectively. By the end of the polymerization, the reaction mixture affording **P1** formed a gellike substance. The gel was dissipated in chloroform; although most materials were dissolved, a small amount of product that was not soluble in an excessive amount of solvent was removed via filtration and discarded. In contrast, the polymerizations of **P2** and **P3** remained soluble throughout the entire reaction, without precipitation or gel formation. **P2** and **P3** were very soluble in a variety of organic solvents, such as chloroform, methylene chloride, tetrahydrofuran (THF), toluene, and dimethylformamide. Their molecular weights (MWs) relative to polystyrene standards were obtained from gel permeation chromatography (GPC) eluting with THF (Table 1). The superior solubility of the larger iptycene scaffolds was reflected by the high (>100 000) MWs of **P2**−**3**. **P1**'s molecular weight is evidently limited by its insoluble nature at higher MW.

Photophysical Characterizations. The photophysical properties of **P1**−**3** were characterized in both solution and the solid state, and the results are summarized in Figure 1 and Table 1. There is great similarity between the thin film and solution absorption and fluorescence spectra of each polymer. The longer wavelength peaks in the emission spectra are assigned to 0−1 vibrational bands and exhibit energy splittings with the emission maximum (0−0 band) of around 1500 and 2150 cm^{-1}, which are the frequencies of carbon−carbon double- and triple-bond vibrations, respectively. Minimal differences are observed between the shape of

Table 1. Molecular Weight and Photophysical Data of Polymers P1−4[a]

polymers	M_n/kDa (PDI)[b]	lifetime τ/ns	quantum yield Φ_F[c]
P1	36 (2.3)[d]	0.28	0.46
P2	124 (2.7)	0.29	0.44
P3	107 (1.9)	0.30	0.50
P4	64 (2.5)	0.51	0.65

[a] MW data are measured in THF relative to polystyrene standards; the lifetime and quantum yields were measured in chloroform. [b] Number-average MW; polydispersity index in parentheses. [c] The quantum yield values were determined using quinine sulfate in 0.1 M sulfuric acid as the standard ($\Phi_F = 0.53$). [d] Part of the product was insoluble, which was removed by filtration, and the molecular weight for the soluble portion was measured.

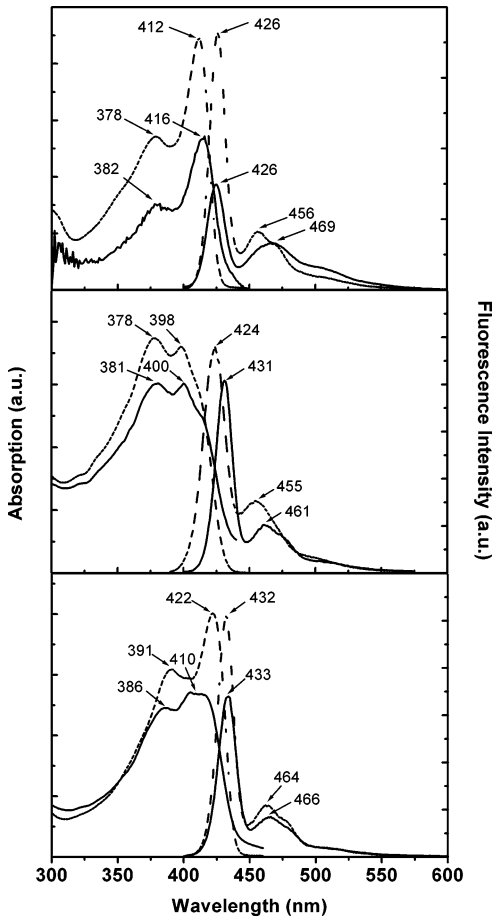

Figure 1. Absorption and fluorescence spectra of **P1** (top), **P2** (middle), and **P3** (bottom) in chloroform (dashed lines) and spin-cast films (solid lines).

P3's solution and solid-state spectra, thereby confirming the effectiveness of its iptycene scaffold to isolate the polymer delocalized backbones. A minor red shift is observed in the emission of **P2**, which is likely due to conformational preferences in thin films. All of the polymers exhibit some emission tailing at longer wavelengths that may be the result of vibrational fine structure or interpolymer interactions. In the film of **P1** this effect is most pronounced and is likely indicative of an emission from a minor species. Regardless of their subtle features, **P1**−**3** are all highly fluorescent in spin-cast thin films, and there is very minimal interpolymer ground-state or excited-state electronic coupling in the solid state. This is distinctively different from what was observed with PPDs that do not contain the iptycene

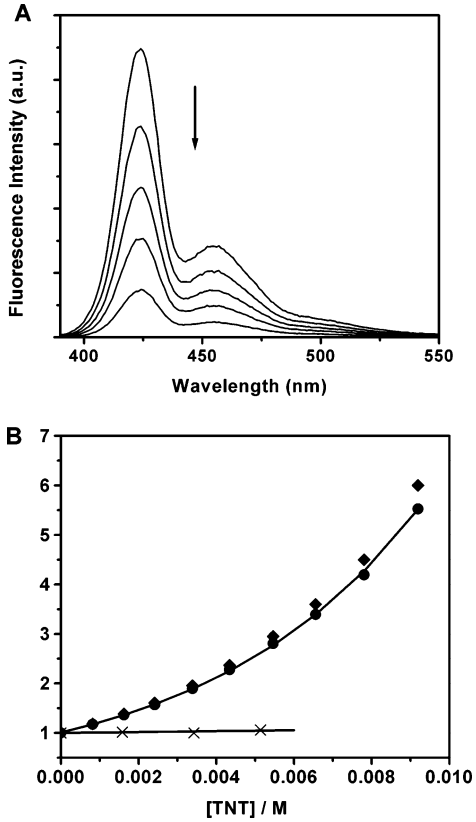

Figure 2. (A) Fluorescence spectra change of **P2** as a function of TNT concentration in chloroform: [**P2**] = 1.2×10^{-6} M; [TNT] = 0−9.2 mM (from top to bottom). (B) Stern−Volmer plot of **P2** in response to TNT: F_0/F (diamond); τ_0/τ (cross); $F_0/F/(1 + K_D[TNT])$ (circle); best fit of experimental data to eqs 2 and 3 (solid lines) with K_D and V determined to be 9 and 185 M^{-1}, respectively.

scaffolds,[8] suggesting that the iptycenes, especially the large ones, are effective for the prevention of detrimental interchain interactions.

Solution Fluorescence Quenching Studies. It is informative to investigate the fluorescence quenching activities of **P1**−**3** in solution. Conducting these studies in chloroform, a good solvent, allows us to evaluate the responses of individual polymer chains and the relative analyte affinities to the polymers under these conditions.

The fluorescence quenching properties of the PPDs were studied by systematically examining the steady-state fluorescence intensity changes in response to four different electron-deficient aromatic compounds: 2,4,6-trinitrotoluene (TNT), 2,4-dinitrotoluene (DNT), 4-nitrotoluene (*p*-NT), and benzophenone (BP). A representative emission profile for **P2** as a function of added TNT is shown in Figure 2A. Similar data were obtained for each quencher for all of the PPDs, and under no cases were any new emission bands observed. Additionally, it has been confirmed that the fluorescence quenching properties of the PPDs are independent of the concentration and MW of the polymers (see the Supporting Information for details). When the relative fluorescence intensity is plotted as a function of quencher concentration (i.e., a Stern−Volmer plot), as shown in Figure 3, two general features are clear. First, all three polymers **P1**−**3** exhibited a consistent trend in their quenching sensitivity toward the four quenchers. Specifically, TNT is the most efficient quencher, followed by DNT and then *p*-NT, and BP is the least effective quencher.

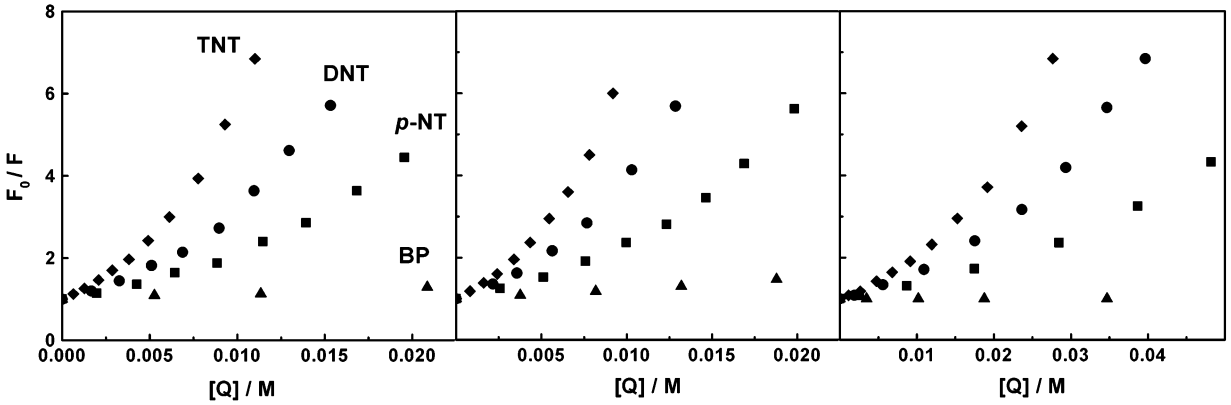

Figure 3. Stern−Volmer plots of **P1** (left), **P2** (middle), and **P3** (right) in chloroform in response to TNT (diamond), DNT (circle), *p*-NT (square), and BP (triangle).

Second, all **P1**−**3** gave rise to nonlinear curves (positive curvatures) in their Stern−Volmer (S−V) plots.

One of the possible reasons for fluorophores to exhibit nonlinear Stern−Volmer plot is that the quenching is a combined result from both dynamic (collisional) and static quenching.[10] Depending on the quenching mechanism, two different equations (eqs 1 and 2) can be used to quantify the experimental data and determine the quenching constants for such complex quenching processes.[10−12]

$$F_0/F = (1 + K_D[Q])(1 + K_S[Q]) \quad (1)$$

$$F_0/F = (1 + K_D[Q])\exp(V[Q]) \quad (2)$$

In these equations, F_0 and F are the fluorescence intensities in the absence and presence of the quencher, respectively, K_D denotes the dynamic quenching constant, and K_S and V represent the static quenching constant. Notably, in eq 1 the term represents the contribution from the static quenching $(1 + K_S[Q])$ is a linear function of quencher concentration [Q], while in eq 2 the corresponding portion, $e^{V[Q]}$, is a nonlinear function of [Q]. When the fluorophore and the quencher form a simple one-to-one dark complex, eq 1 can be derived.[10] In such cases, K_S corresponds to the association constant of the fluorophor−quencher complex. However, for systems with more complex species the quenching profile may deviate from the linear function, and the more general form of equation (i.e., eq 2) can be used.[12−14] Additionally, eq 1 can be viewed as an approximation of eq 2 when [Q] or K_S (or V) is very small. The two equations are thus applied to different systems in accordance with the experimental results.

The fluorescence lifetime is truncated by collisional quenching but unaffected by static quenching.[10] As a result, monitoring the lifetime changes represents the conventional practice for determining the dynamic quenching constant independent of the static quenching process. The correlation of lifetime with quencher concentration can be expressed as

$$\tau_0/\tau = 1 + K_D[Q] \quad (3)$$

The fluorescence lifetimes of **P1**−**3** were therefore measured in the presence of a series of concentrations of different quenchers. By fitting the lifetime data to eq 3, dynamic quenching constants K_D were determined. Subsequently applying K_D to eq 2 (eq 2 instead of eq 1 was used because of the nonlinear relationship between $(F_0/F)/(1 + K_D[Q])$ and [Q] observed in our systems) allows the determination of the static constant V. An example of this data analysis process is shown in Figure 2B (see the SI for more data and plots), and the quenching constants thereby obtained are summarized in Table 2. Generally, polymers **P1**−**3** exhibited minimal values of dynamic quenching constants, and in some cases no detectable lifetime change was observed. Namely, static quenching is the dominant mechanism for all PPD polymers and quenchers in our current investigations. For all three PPDs the static quenching constant diminishes in the order of TNT, DNT, *p*-NT, and BP for a given polymer (Table 2 and the SI).

Table 2. Quenching Constant Data of Polymers P1−3[a]

	$V(K_D)/M^{-1}$			
polymers	TNT	DNT	*p*-NT	BP
P1	166 (10)	112 (4)	74 (<1)	13 (<1)
P2	185 (9)	135 (<1)	86 (<1)	21 (<1)
P3	64 (6)	49 (<1)	30 (<1)	1.0 (<1)

[a] All quenching constants were determined in $CHCl_3$ by fitting the experimental data to eqs 2 and 3. Static quenching constants V are listed in the table with dynamic quenching constants K_D shown in parentheses. When no lifetime change was observed within instrumentation error, K_D is reported as <1 and was assumed negligible in determining corresponding static quenching constant V.

The quenching sensitivities of PPD polymers were compared to a PPE polymer, **P4**, using DNT as the representative quencher. As seen from Figure 4, in solution all **P1**−**3** manifested higher quenching sensitivity toward DNT than **P4**. Furthermore, lifetime studies revealed that, unlike PPDs, the quenching of **P4** by DNT arises from more balanced contributions from dynamic and static mechanisms. Specifically, by applying the steady-state intensity and lifetime data of **P4** to eqs 2 and 3, a dynamic quenching constant $K_D = 18\ M^{-1}$ and a static quenching constant $V = 26\ M^{-1}$ were obtained. Interestingly, the dynamic constant was considerably larger than those of **P1**−**3**, but the static quenching efficiency was significantly lower. This latter point suggests that the more structurally restricted environment about the PPDs does not allow the quencher close enough proximity to the polymer backbone by simple diffusion. Put differently, for the quenchers to be close enough to quench the polymer they are in such intimate contact as to be effectively "bound" to the polymer in a static complex. This is further alluded to by our speculation that intimate contact between the quencher and the aromatic units in the conjugated

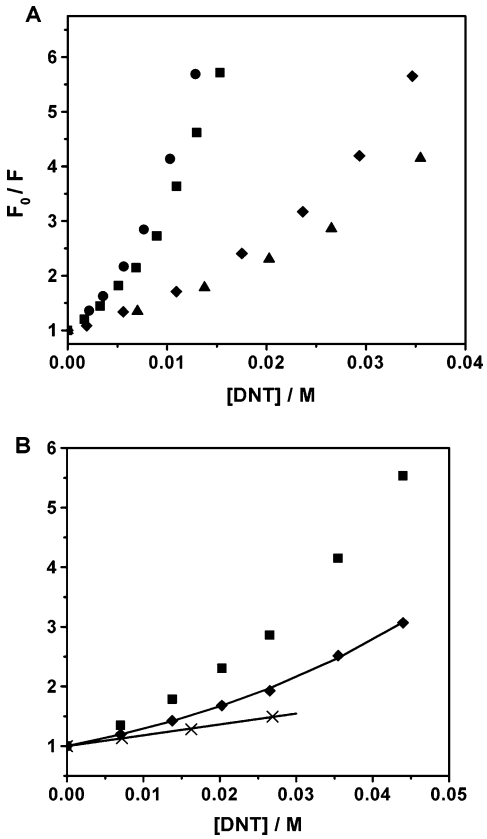

Figure 4. (A) Stern−Volmer plots of **P1** (square), **P2** (circle), **P3** (diamond), and **P4** (triangle) in chloroform in response to DNT. (B) The Stern−Volmer plot of **P4** in response to DNT: F_0/F (square); τ_0/τ (cross); $F_0/F/(1 + K_D[DNT])$ (diamond); best fit of experimental data to eqs 2 and 3 (solid lines) with K_D = 18 M^{-1} and V = 26 M^{-1}.

backbone, most likely in a cofacial fashion, is largely responsible for the quenching. Further evidence supporting this viewpoint is given by the even lower K_D found in **P2** and **P3** compared to that of **P1** (Table 2). It follows that the larger iptycenes are more effective in "shielding" the backbone.

It is also interesting that the much larger static quenching constants exhibited by the PPDs suggested significant ground-state associations between these polymers and the quenchers. This enhanced polymer−quencher complexation is attributed to the stronger tendency of the electron-rich dialkoxyphenyl rings, relative to the other unadorned phenyl rings, to associate with electron-deficient quenchers via electrostatic and/or $\pi-\pi$ stacking interactions. This postulation is supported by the correlation of the quenching efficiency with the structure of the quenchers; i.e., the more electron-deficient the quencher, the higher affinity for binding the polymers, the larger the quenching constant (Table 2). Moreover, the trend of the quenchers' abilities to form π-stacking complexes coincides with their relative electron affinity, i.e., lower LUMO that are presumably involved in the charge-transfer process.[1,5,15]

Another conspicuous feature of the S−V plots of the PPD polymers is the nonlinear relationship between $(F_0/F)/(1 + K_D[Q])$ and [Q]. Such upward curvatures in the S−V plot are not uncommon for fluorescent conjugated polymers.[14,16,17] However, in most previous cases, they involved electrostatic interactions between polyelectrolytes and quenchers bearing opposite charges, and a "sphere-of-action" model was invoked. The strong hydrophobic backbones in these other systems and the strong associations with the charged quenchers or other biomolecules suggest that some of the polyelectrolyte results involved significant changes in polymer conformations and potentially aggregation.[3e] Hence, in these earlier studies the strong upward curvatures could also be explained by enhancements in the binding constants resulting from analyte-induced conformational and/or aggregation changes. However, the polymers and the quenchers in the current studies are not ionic species, and the concentration-independent quenching property (see Figure S5) has suggested that the interpolymer aggregation is not the cause for the nonlinear behavior. Moreover, their quenching behaviors are not the result of a "sphere of action", since the static quenching constant V (corresponding to the "sphere-of-action" volume) of a given polymer significantly changes with quenchers. The large values of V clearly imply some specific associations between the polymers and the quenchers, which can be ascribed to the electrostatic and π-stacking interactions (vide supra). These effects reveal the additional complexities of fluorescence quenching of conjugated polymers, and a number of factors including the kinetics of the association/dissociation of the quencher with the polymer, electron/energy transfer between the quencher and the polymer, the rate of exciton migration along the polymer backbone,[18] and the fact that binding of analytes can affect the polymer conformation, which in turn controls its properties. For the current systems, once a quencher is bound to the polymer, most likely to the nonconjugated electron-rich dialkoxyphenyl rings, electron/energy transfer between the conjugated backbone and the quencher causes nonradiative relaxation of excitons. The rapid migration of excitons confers the enhanced quenching and quenching can occur by electron transfer or energy transfer to a charge-transfer complex by Dexter and/or Forster mechanisms.[19] The nonlinear relationship between the static quenching efficiency $(F_0/F)/(1 + K_D[Q])$ is likely the result of a confluence of multiple effects.

The role of the elaborated iptycenes is most impressively revealed by the differences in the quenching sensitivities (Table 2) of **P2** and **P3**, which are formally stereoisomers of each other. Although **P2** exhibited slightly higher quenching sensitivity relative to **P1**, which incorporates a smaller iptycene, **P3** displayed much lower quenching constants for each quencher examined (representative data shown in Figure 4A, see also the SI). As the electronic properties of **P2** and **P3** are similar, the difference in their quenching behaviors is related to the stereo-configurations of the iptycenes. This observation supports the notion that the quenchers interact with the aromatic units of the iptycenes, and consequently the configuration of the iptycences strongly influences the quenching sensitivity.

Fluorescence Quenching in the Solid State. Studies of the solid-state quenching properties of PPD polymers focused on TNT and DNT because they provide rapid and large-amplitude responses that are convenient to monitor. Polymer thin films on glass cover slides were prepared from chloroform solutions of the polymers by a conventional spin-casting technique. A small amount of solid TNT or DNT was placed in a quartz cell with cover. The cell was equilibrated for multiple hours to ensure saturation vapor pressure had been reached. The cell was placed in the emission spectrometer, and then the coated cover slide was

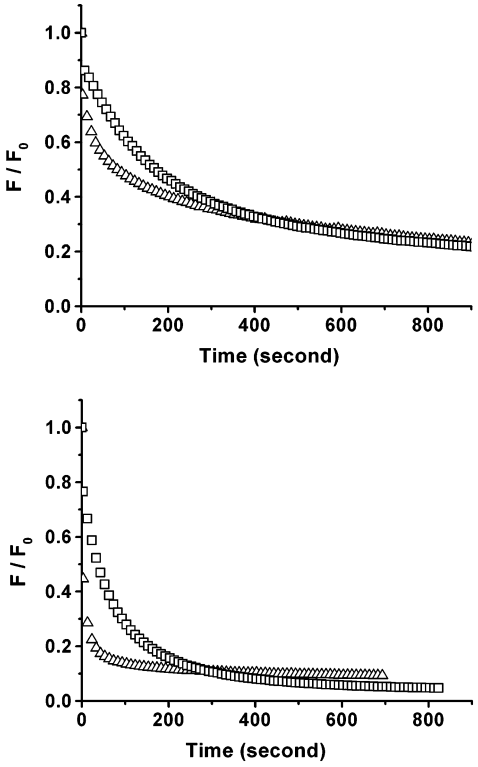

Figure 5. Fluorescence quenching of **P2** (top) and **P4** (bottom) in spin-cast thin films upon being exposed to TNT (square) and DNT (triangle) vapor.

carefully positioned in the cell such that it was only exposed to the analyte vapor but not in direct contact with the solid quencher. The recording of the fluorescence change was started immediately after the film was put in the cell. The fluorescence intensities were normalized to the original values recorded before the films were exposed to the quencher vapor, and the change was measured over time. Representative data of **P2** and **P4** are plotted in Figure 5. **P1** and **P3** behaved very similarly to **P2** (shown in the SI).

The results from these experiments can be summarized as follows. In the thin films, PPD polymers (**P1**−**3**) were quenched at a slower rate by both TNT and DNT compared to the PPE (**P4**).[20] These results contrast with the solution results, in which PPDs showed overall higher quenching sensitivities toward these analytes. Clearly, the solid-state behaviors are governed by different factors than those determined in solution.[21]

Real-Time Fluorescence Quenching and Recovery. Quenching studies on spin-cast films provided important information on the quenching kinetics of the polymers in the solid state. It was noticed during these studies that it took a much longer period of time for **P1**−**3** to regain their fluorescence than PPE **P4**. To examine these effects in greater detail, a Fido[22] sensor device was employed to obtain real-time information on the fluorescence recovery of these polymers.

The sample preparation for a Fido device involves spin-casting polymer thin films onto the surface inside glass capillaries (i.d. = 0.6 mm). These capillaries are then mounted into a Fido sensor wherein a constant air flow of 35 mL/min is passed through the capillary. When the air inlet is contaminated by a given quencher vapor, the polymer's fluorescence response is monitored. After the quencher vapor source is removed, analyte-free air continues to flow through the capillary. Our experiments in the emission spectrometer were done under static atmosphere, and consequently the fluorescence responses and recoveries are faster in Fido.

The fluorescence quenching and recovery profiles of **P1**, **P2**, and **P4** recorded by Fido are shown in Figure 6 (see the SI for results from **P3**, which displayed very similar behavior to **P2**). The fluorescence intensities are normalized to be 100% on the scale before the quencher vapor was introduced. For DNT quenching (Figure 6A−C), the exposure to ∼0.1 ppm of DNT was for 2 s, and the fluorescence responded instantly for all polymers. The fluorescence recovery after removal of the quencher vapor varied depending on the polymers. The DNT quenching of **P4** was reversible with nearly complete fluorescence recovery within seconds after removal of the quencher vapor. In contrast, the fluorescence recoveries of **P2** and **P3** were much slower, and the intensity was only partially regained after a few minutes. The behavior of **P1** was between the two extremes presented by **P2** and **P4**. The slower fluorescence recovery displayed by PPDs is consistent with the conclusions drawn from solution studies. That is, strong binding interactions exist between the PPD polymers and the quenchers. These binding forces retard the escape of quencher molecules from the polymers, resulting in slow fluorescence recovery or even seemingly irreversible quenching. Additionally, that fact that **P1** recovered its fluorescence more readily than **P2** and **P3** suggests that the pore size within the materials is another important factor that determines the efficacy of the polymers in sequestering the quencher molecules.

Despite the lower vapor pressure of TNT (5−7 ppb), all the polymers were most sensitive to TNT quenching. The exposure time of TNT had to be limited to less than a second because slightly longer exposure time (>1 s) would cause the fluorescence intensity of any polymer to drop to 0% and take an extremely long time to recover. The varied quenching amplitude shown in Figure 6F was a result of manually controlled exposure time, which is difficult with such fast time constants. As can be seen from Figure 6, **P1** behaved similarly to **P2** in response to TNT, i.e., very slow in fluorescence recovery. Again, responses from **P2** and **P3** were similar. An observation that particularly caught our attention for TNT quenching was that, despite the short exposure time (<1 s), the fluorescence intensity of **P2** continued to drop long after (≈2 min) the quencher vapor was removed before it reached the minimum and started to recover very slowly. Similar observations were also made for **P1** and **P3**, only to a lesser extent. These particularly slow quenching processes are believed to be due to the unique quencher-sequestering property of these iptycene-containing polymers. The capillaries used in Fido are about 8 cm long although only a portion of the polymer is excited within the capillary. The capillary effectively displays chromatographic behavior, and a very small amount of TNT could be repeatedly adsorbed and desorbed from the polymer as it travels along the capillary before it could reach the area where the polymer is excited and the fluorescence emission is monitored. If the polymer material is able to sequester the quencher molecule very efficiently, a "delayed" quenching will emerge. An alternate explanation for the slow quenching is that the analyte molecules are mostly trapped in the thin layer on the surface due to the strong binding with the polymer, and it takes time for them to

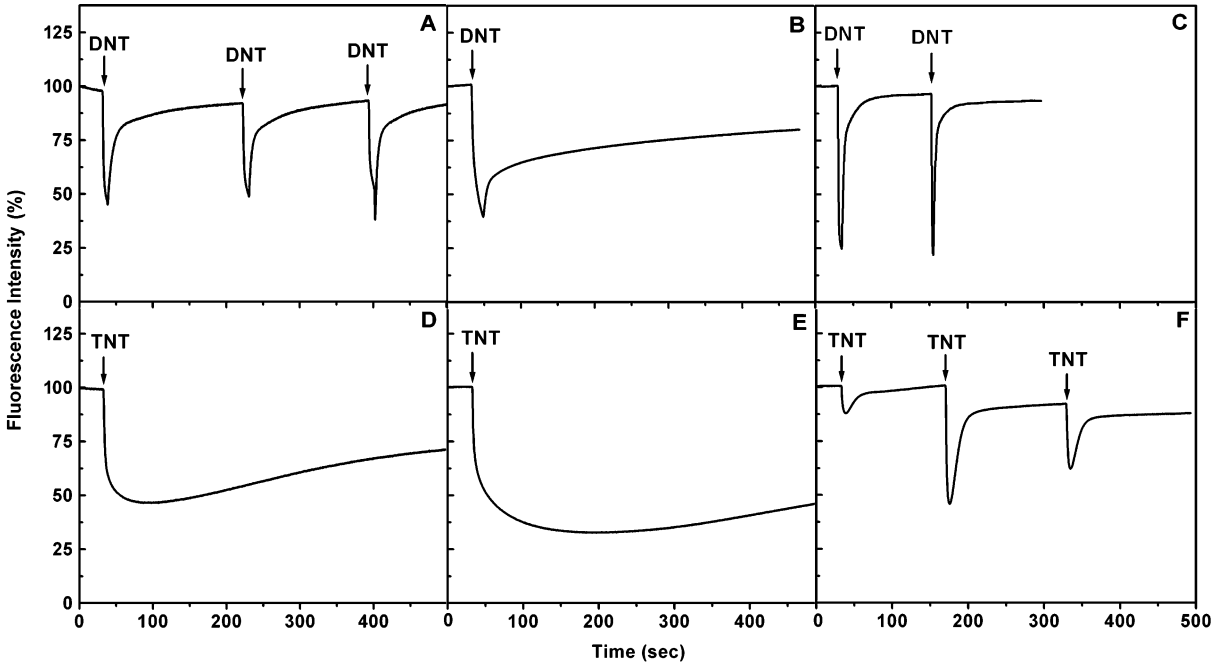

Figure 6. Real-time fluorescence intensity profiles (quenching followed by recovery) of **P1** (A, D), **P2** (B, E), and **P4** (C, F) in response to DNT (top) or TNT vapor (bottom). The arrows indicate the points when quencher vapor was introduced. The exposure time for DNT is ca. 2 s and <1 s for TNT.

diffuse deeper into the polymer films.[5] Given the greater affinity for TNT and DNT by PPDs, it is interesting to consider why **P4** displays greater sensitivity. Tight binding to the surfaces of the films may be a problem as if molecules pile up in one site they cannot effectively quench as much of the polymer as if they were distributed more uniformly. In addition, there is the likely possibility that the greater spacing between the polymer chromophores (i.e., the backbones) leads to reduced rates for interchain energy migration. This effect will limit the amplification achieved by this method.

Conclusion

A new series of poly(*p*-phenylenebutadiynylene)s (PPDs) have been synthesized. In these polymers, each *p*-phenylene unit in the conjugated backbone is the core group of a rigid three-dimensional iptycene scaffold. These polymers manifested sensitive fluorescence quenching activities in response to a series of electron-deficient aromatic molecules in both solution and the solid state. In solution the PPDs displayed a higher sensitivity toward the studied quenchers than a PPE polymer. Static quenching was the dominant quenching mechanism in solution for the PPDs, and dynamic quenching only played a negligible role. In contrast, the PPE exhibited comparable dynamic and static quenching constants under similar conditions. Additionally, the configuration of the iptycences incorporated in the polymer was shown to strongly influence the quenching behavior.

For solid-state quenching, a real-time fluorescence sensory device was employed, in addition to the conventional fluorescence spectrometer, to study both the fluorescence quenching and recovery processes. The results indicated that different factors dominate in the solid-state sensitivity than those observed in solution. Our results also suggest that PPDs having large iptycene scaffolds that introduce porosity exhibited enhanced ability in retaining the quencher molecules. Hence, structures like these may be of interest as analyte preconcentrators for trace analyte detection.

The profound differences in the solution and solid-state (thin) film quenching effects in the PPDs and PPEs also draw attention to the fact that care must be taken in making comparisons of sensitivities. This is highlighted by recent reports of silole polymers that displayed 3.7 times greater sensitivity than **P4** to TNT in toluene solution.[23] However, these same materials displayed only 8.2% quenching in a continuous flow of TNT vapor after 10 min. When compared to ≈50% quenching by **P4** in less than 1 s exposure, it can be revealed that in a sensory device the silole polymers are more than 1000 times less sensitive in thin film form.[24]

Acknowledgment. This research was supported by the Army Research Office through the Institute for Soldier Nanotechnologies, TSA and TSWG.

Supporting Information Available: Syntheses of **P1**−**3** and more data from fluorescence quenching studies in solution and the solid state. This material is available free of charge via the Internet at http://pubs.acs.org.

References and Notes

(1) Swager, T. M. *Acc. Chem. Res.* **1998**, *31*, 201−207.
(2) McQuade, D. T.; Pullen, A. E.; Swager, T. M. *Chem. Rev.* **2000**, *100*, 2537−2574.
(3) For recent examples of fluorescent conjugated polymer based sensors: (a) Wosnick, J. H.; Mello, C. M.; Swager, T. M. *J. Am. Chem. Soc.* **2005**, *127*, 3400−3405. (b) Pinto, M. R.; Schanze, K. S. *Proc. Natl. Acad. Sci. U.S.A.* **2004**, *101*, 7505−7510. (c) Kumaraswamy, S.; Bergstedt, T.; Shi, X.; Rininsland, F.; Kushon, S.; Xia, W.; Ley, K.; Achyuthan, K.; McBranch, D.; Whitten, D. *Proc. Natl. Acad. Sci. U.S.A.* **2004**, *101*, 7511−7515. (d) Dore, K.; Dubus, S.; Ho, H.-A.; Levesque, I.; Brunette, M.; Corbeil, G.; Boissinot, M.; Boivin, G.; Bergeron, M. G.; Boudreau, D.; Leclerc, M. *J. Am. Chem. Soc.* **2004**, *126*, 4240−4244. (e) Wang, S.; Gaylord, B. S.; Bazan, G. C. *J. Am. Chem. Soc.* **2004**, *126*, 5446−6451. (f) Huang, H.; Wang, K.; Tan, W.; An, D.; Yang, X.; Huang, S.; Zhai, Q.; Zhou, L.; Jin, Y. *Angew. Chem., Int. Ed.* **2004**, *43*, 5635−5638.

(4) (a) Zhou, Q.; Swager, T. M. *J. Am. Chem. Soc.* **1995**, *117*, 7017−7018. (b) Zhou, Q.; Swager, T. M. *J. Am. Chem. Soc.* **1995**, *117*, 12593−12602.
(5) (a) Yang, J.-S.; Swager, T. M. *J. Am. Chem. Soc.* **1998**, *120*, 5321−5322. (b) Yang, J.-S.; Swager, T. M. *J. Am. Chem. Soc.* **1998**, *120*, 11864−11873.
(6) Amara, J. P.; Swager, T. M. *Macromolecules* **2004**, *37*, 3068−3070.
(7) (a) Bashir-Hashemi. A.; Hart, H.; Ward, D. L. *J. Am. Chem. Soc.* **1986**, *108*, 6675−6679. (b) Chen, Y. S.; Hart, H. *J. Org. Chem.* **1989**, *54*, 2612−2615. (c) Venugopalan, P.; Burgi, H.-B.; Frank, N. L.; Baldridge, K. K.; Siegel, J. S. *Tetrahedron Lett.* **1995**, *36*, 2419−2422.
(8) Williams, V. E.; Swager, T. M. *J. Polym. Sci., Part A: Polym. Chem.* **2000**, *38*, 4669−4676.
(9) **M3** is a mixture of two stereoisomers (ca. 1:1 molar ratio); syntheses of **M1**−**3** are reported elsewhere: Zhao, D.; Swager, T. M., submitted for publication.
(10) *Principles of Fluorescence Spectroscopy*, 2nd ed.; Lakowicz, J. R., Ed.; Kluwer Academic/Plenum Publishers: New York, 1999.
(11) Frank, J. M.; Wawilow, S. J. *Z. Phys.* **1931**, *69*, 100−110.
(12) Eftink, M. R.; Ghiron, C. A. *J. Phys. Chem.* **1976**, *80*, 486-493.
(13) Eftink, M. R.; Ghiron, C. A. *Anal. Biochem.* **1981**, *114*, 199−227.
(14) Wang, J.; Wang, D.; Miller, E. K.; Moses, D.; Bazan, G. C.; Heeger, A. J. *Macromolecules* **2000**, *33*, 5153−5158. (b) Wang, D.; Wang, J.; Moses, D.; Bazan, G. C.; Heeger, A. J. *Langmuir* **2001**, *17*, 1262−1266.
(15) *Handbook Series in Organic Electrochemistry*; Meites, L., et al., Eds.; CRC Press: Boca Raton, FL, 1978; Vol. 1.
(16) Ramey, M. B.; Hiller, J.; Rubner, M. F.; Tan, C.; Schanze, K. S.; Reynolds, J. R. *Macromolecules* **2005**, *38*, 234−243.
(17) Murphy, C. B.; Zhang, Y.; Troxler, T.; Ferry, V.; Martin, J. J.; Jones, W. E. *J. Phys. Chem. B* **2004**, *108*, 1537−1543.
(18) Itoh, Y.; Kamioka, K.; Webber, S. E. *Macromolecules* **1989**, *22*, 2851−2852.
(19) In the current particular system the absence of quenching via energy transfer mechanism is suggested by the absence of lower energy band in the UV−vis spectra of **P1**−**3** upon long exposures to TNT vapor.
(20) The slower responses to TNT than to DNT are most likely due to the much lower vapor pressure of TNT. For vapor pressure values, see ref 5 and *Handbook of Physical Organic Chemicals*; Howard, P. H., Meylan, W. M., Eds.; CRC Press: Boca Raton, FL, 1997.
(21) This contrasting behavior between the solution and thin films is in accord with differences that we have observed other systems. Kim, Y.; Zhu, Z.; Swager, T. M. *J. Am. Chem. Soc.* **2004**, *126*, 452−453.
(22) Fido is a commercial sensory device marketed by Nomadics Inc.
(23) Sohn, H.; Sailor, M. J.; Magde, D.; Trogler, W. C. *J. Am. Chem. Soc.* **2003**, *125*, 3821−3830.
(24) Sohn, H.; Calhoun, R. M.; Sailor, M. J.; Magde, D.; Trogler, W. C. *Angew. Chem., Int. Ed.* **2001**, *40*, 2104−2105.

MA051584Y